

# ISO observations of the Wolf-Rayet galaxy NGC 7714 and its companion NGC 7715

B.O'Halloran<sup>1</sup>, L. Metcalfe<sup>2</sup>, M. Delaney<sup>1</sup>, B. McBreen<sup>1</sup>, R. Laureijs<sup>2</sup>, K. Leech<sup>2</sup>, D. Watson<sup>1</sup> and L. Hanlon<sup>1</sup>

<sup>1</sup> Physics Department, University College, Belfield, Dublin 4, Ireland

<sup>2</sup> ISO Data Centre, Astrophysics Division, Space Science Department of ESA, Villafranca, P.O. Box 50727, E-28080 Madrid, Spain

Received 14 April 2000 / Accepted 7 June 2000

**Abstract.** The interacting system Arp 284 consisting of the Wolf-Rayet galaxy NGC 7714 and its irregular companion NGC 7715 was observed using the Infrared Space Observatory. Deconvolved ISOCAM maps of the galaxies using the 14.3  $\mu\text{m}$ , 7.7  $\mu\text{m}$  and 15  $\mu\text{m}$  LW3, LW6 and LW9 filters, along with ISOPHOT spectrometry of the nuclear region of NGC 7714 were obtained and are presented. Strong ISOCAM emission was detected from the central source in NGC 7714, along with strong PAH features, the emission line [Ar II], molecular hydrogen at 9.66  $\mu\text{m}$  and a blend of features including [S IV] at 10.6  $\mu\text{m}$ . IR emission was not detected from the companion galaxy NGC 7715, the bridge linking the two galaxies or from the partial stellar ring in NGC 7714 where emission ceases abruptly at the interface between the disk and the ring.

The morphology of the system can be well described by an off-centre collision between the two galaxies. The LW3/LW2, where the LW2 flux was synthesized from the PHOT-SL spectrum, LW9/LW6 and LW3/LW6 ratios suggest that the central burst within NGC 7714 is moving towards the post-starburst phase, in agreement with the age of the burst. Diagnostic tools including the ratio of the integrated PAH luminosity to the 40 to 120  $\mu\text{m}$  infrared luminosity and the far-infrared colours reveal that despite the high surface brightness of the nucleus, the properties of NGC 7714 can be explained in terms of a starburst and do not require the presence an AGN.

**Key words:** galaxies individual - NGC 7714 - NGC 7715 - galaxies interactions - galaxies starburst

## 1. Introduction

Wolf-Rayet galaxies are a subset of emission line and H II galaxies whose integrated spectra have a broad emission feature around 4650Å which has been attributed to Wolf-Rayet stars. The emission feature usually consists of

a blend of lines namely, HeI  $\lambda$ 4686, CIII/CIV  $\lambda$ 4650 and NIII  $\lambda$ 4640. The CIV  $\lambda$ 5808 line can also be an important signature of Wolf-Rayet activity. Wolf-Rayet galaxies are important in understanding massive star formation and starburst evolution (Schaerer & Vacca, 1998; Mas-Hesse & Kunth, 1999). The Wolf-Rayet phase in massive stars is short lived and hence gives the possibility of studying an approximately coeval sample of starburst galaxies (Metcalfe et al., 1996; Rigopoulou et al., 1999). The first catalog of Wolf-Rayet galaxies was compiled by Conti (1991) and contains 37 galaxies. A large number of additional Wolf-Rayet galaxies have been identified and a new catalog containing 139 galaxies has been compiled by Schaerer et al. (1999).

The interacting system Arp 284 consists of an active starburst galaxy NGC 7714 and its post starburst companion NGC 7715. This system has been the subject of several investigations (Demoulin et al., 1968; Weedman et al., 1981) because of its unusual morphology. Van Breugel et al. (1985) first reported weak Wolf-Rayet features near 4846 Å, and possible HeII emission from the nucleus of NGC 7714. NGC 7714 is an SBb peculiar galaxy and classified by Weedman et al. (1981) as a proto-typical starburst. The heliocentric radial velocity is 2798 km s<sup>-1</sup> which places it at a distance of 37.3 Mpc assuming  $H_0 = 75 \text{ km s}^{-1} \text{ Mpc}^{-1}$  (Gonzalez-Delgado et al., 1994). The spectrum from X-rays (Stevens & Strickland, 1998) to VLA radio (Smith & Wallin, 1992) at 6 and 20 cm, was explained as a result of intense star formation in the nucleus (Weedman et al., 1981). Very detailed studies have been carried out in the ultraviolet, optical and near infrared to quantify the gas properties in the nuclear and circumnuclear regions (Weedman et al., 1981; Gonzalez-Delgado et al., 1994; Garcia-Vargas et al., 1997). Hubble Space Telescope (HST) spectroscopy of the nuclear starburst revealed Wolf-Rayet features in the ultraviolet and indicate a population of about 2000 Wolf-Rayet stars (Garcia-Vargas et al., 1997). The B-magnitude of the galaxy is -20.04 and far-infrared luminosity of  $2.8 \times 10^{10} L_{\odot}$  with IRAS far-infrared flux ratios  $f_{60}/f_{100}$  and

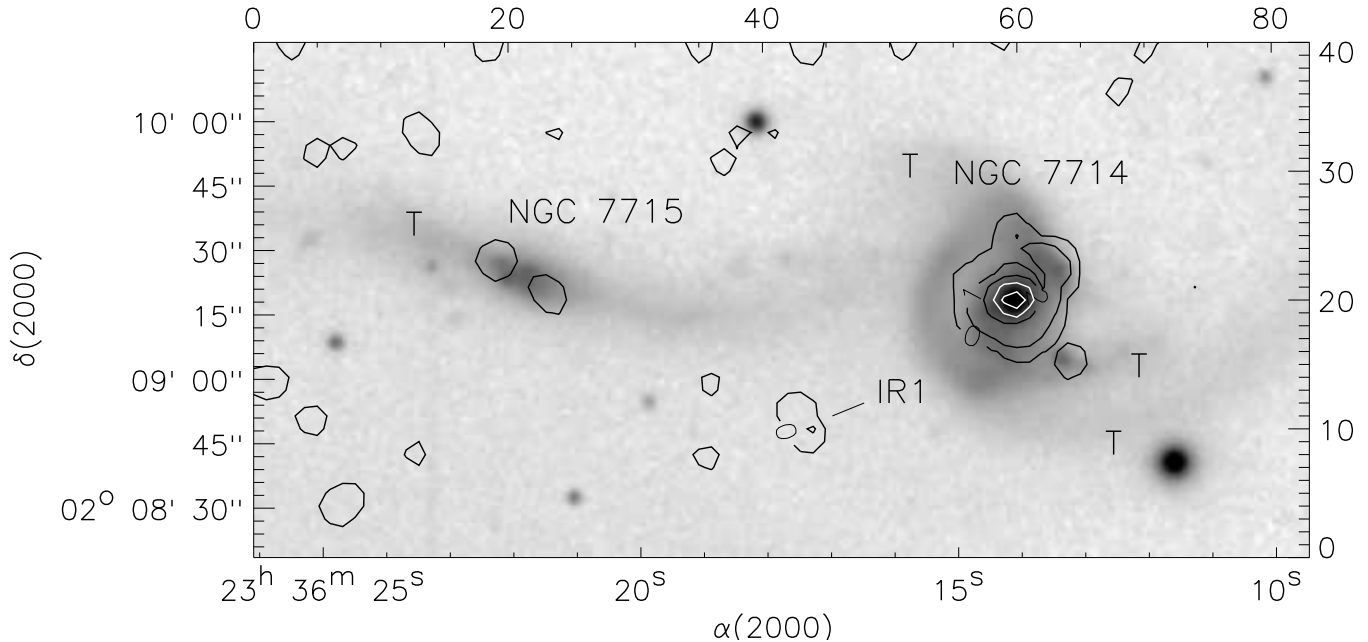


**Fig. 1.** Deconvolved 15  $\mu\text{m}$  LW3 map of NGC 7714 and NGC 7715 overlaid on an R band CCD image, showing the bridge between the two galaxies. Features denoted by 'T' give the positions of tails/arms emanating from both galaxies. Sources coinciding with NGC 7715 were determined to be glitches using robust deglitching techniques. An enlarged view of the NGC 7714 region is given in Figure 2. IR1 is a weak source without an identified optical counterpart.

$f_{25}/f_{60}$  of 0.9 and 0.25 respectively. These ratios indicate that NGC 7714/7715 almost qualifies as a 60  $\mu\text{m}$  peaker source (Heisler et al., 1996; Laureijs et al., 2000).

We present Infrared Space Observatory (ISO) observations of the Arp 284 system containing the interacting galaxies NGC 7714/7715 as part of a program investigating several galaxies exhibiting Wolf-Rayet signatures. The observations and data reduction are presented in Sect. 2. The results are contained in Sect. 3 and discussed in Sect. 4. The conclusions are summarised in Sect. 5.

## 2. Observations and Data Reduction

The ISO observations were obtained using the mid-infrared camera ISOCAM (Cesarsky et al., 1996) and the spectrometric mode of the ISO photopolarimeter ISOPHOT (Lemke et al., 1996). The astronomical observing template (AOT) used was CAM 01, for the raster observations and PHOT40, for spectrometry. The log of the CAM01 observations using the LW3, LW6 and LW9 filters and the PHOT40 observations are presented in Table 1.

### 2.1. ISOCAM

Each observation had the following configuration: 3'' pixel field of view (PFOV), integration time of 5.04 s with a  $5'' \times 2''$  raster, 48'' stepsize, excluding discarded stabilization readouts (Siebenmorgen et al., 1999). All data processing was performed with the CAM Interactive Analysis (CIA) system (Ott et al., 1997; Delaney, 1998), and the

following method was applied during data processing. (i) Dark subtraction was performed using a dark model with correction for slow drift of the dark current throughout the mission. (ii) Glitch effects due to cosmic rays were removed following the method of Aussel et al. (1999). (iii) Transient correction for flux attenuation due to the lag in the detector response was performed by the method described by Abergel et al. (1996). (iv) The raster map was flat-fielded using a library flat-field. (v) Pixels affected by glitch residuals and other persistent effects were manually suppressed. (vi) The raster mosaic images were deconvolved with a multi-resolution transform method described by Starck et al. (1998). The duration of the observations in Table 1 give the length of the actual observation including instrumental, but not spacecraft, overheads. Photometry was performed by integrating the pixels containing source flux exceeding the background by  $3\sigma$ . Contour levels are based on a power scale, where the lowest level is approximately 2 times the standard deviation, or  $\sigma$ , of the background noise, using pixels from around the border of the image.

### 2.2. PHOT-S

PHOT-S consists of a dual grating spectrometer with a resolving power of 90. Band SS covers the range 2.5 - 4.8  $\mu\text{m}$ , while band SL covers the range 5.8 - 11.6  $\mu\text{m}$ . (Laureijs et al., 1998). The PHT-S spectra of NGC 7714 was obtained by pointing the  $24'' \times 24''$  aperture of PHT-S alternatively towards the peak of the LW6 emission (for

**Table 1.** Log of the ISO observations of NGC 7714 and NGC 7715. The nine columns list the observation name, the AOT, the filter, the wavelength range ( $\Delta\lambda$ ), the reference wavelength of the filter, the date and duration of the observation, and the position of the observation in RA and declination respectively.

Observation	AOT#	filter	$\Delta\lambda$ ( $\mu\text{m}$ )	$\lambda_{\text{ref}}$ ( $\mu\text{m}$ )	date	duration (seconds)	Right Ascension (RA)	Declination (Dec)
NGC7714	CAM01	LW3	12–18	14.3	24 May 1997	1936	23h 36m 18s	+02° 09' 18"
NGC7714	CAM01	LW6	7–8.5	7.7	24 May 1997	1938	23h 36m 18s	+02° 09' 18"
NGC7714	CAM01	LW9	14–16	15	27 May 1997	1936	23h 36m 18s	+02° 09' 18"
NGC7714	PHT40	SS/SL	2.5–11.6		24 May 1997	1132	23h 36m 14s	+02° 09' 18"
NGC7715	PHT40	SS/SL	2.5–11.6		24 May 1997	1132	23h 36m 22s	+02° 09' 25"

**Table 2.** ISOCAM and IRAS fluxes for NGC 7714. The four columns list the filter used, the wavelength range, the reference wavelength for the filter and the flux measured. The fluxes have a photometric accuracy of about 15%. IRAS fluxes for NGC 7714 are also given for comparison (Moshir et al., 1990).

filter	$\lambda$ ( $\mu\text{m}$ )	$\lambda_{\text{ref}}$ ( $\mu\text{m}$ )	flux (Jy)
LW3	12.0–18.0	14.3	$0.46 \pm 0.07$
LW6	7.0–8.5	7.7	$0.35 \pm 0.05$
LW9	14–16	15	$0.55 \pm 0.08$
IRAS 12 $\mu\text{m}$	8.5–15	12	$0.47 \pm 0.05$
IRAS 25 $\mu\text{m}$	19–30	25	$2.85 \pm 0.26$
IRAS 60 $\mu\text{m}$	40–80	60	$10.36 \pm 1.24$
IRAS 100 $\mu\text{m}$	83–120	100	$11.51 \pm 0.69$

512 seconds) and then towards two background positions off the galaxy (256 seconds each), using the ISOPHOT focal plane chopper. The calibration of the spectrum was performed by using a spectral response function derived from several calibration stars of different brightness observed in chopper mode (Acosta-Pulido et al., 1999). The relative spectrometric uncertainty of the PHOT-S spectrum is about 20% when comparing different parts of the spectrum that are more than a few microns apart. The absolute photometric uncertainty is about 30% for bright calibration sources. All data processing was performed using the ISOPHOT Interactive Analysis system, version 8.1 (Gabriel, 1998). Data reduction consisted primarily of the removal of instrumental effects. Once the instrumental effects have been removed, background subtraction was performed and flux densities were obtained. These fluxes were plotted to obtain the spectrum for NGC 7714.

### 3. Results

A deconvolved LW3 map overlaid on a R band CCD image (Papaderos & Fricke, 1998) of Arp 284 is presented in Fig.1. Deconvolved maps obtained using the LW3, LW6 and LW9 filters, overlaid on a R band CCD image (Pa-

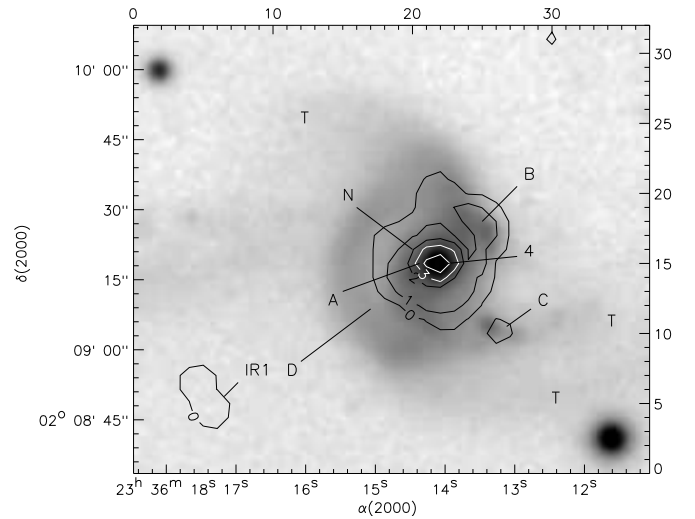


**Fig. 2.** Deconvolved LW3 map of NGC 7714, superimposed on a R band CCD image. The three giant H II regions are marked A, B and C. D is the partial ring and N denotes the nucleus with the Wolf-Rayet signature. The contour levels ( $\text{mJy}/\text{arcsec}^{-2}$ ) are: 0 = 0.1, 1 = 1.0, 2 = 7.0, 3 = 20.0, 4 = 40.0. IR1 is a weak source without an identified optical counterpart.

paderos & Fricke, 1998), are presented in Figs. 2, 3 and 4. It is evident that the strong compact source on each map coincides with the nuclear region of NGC 7714. Three giant H II regions, labelled A, B and C were detected in all three maps, with A lying close to the nucleus, and B and C to the northwest and southwest of the nuclear region (Garcia-Vargas et al., 1997). It is interesting to note that apart from a slight spur of LW6 emission, the bright optical ring to the east of the nucleus was not detected, with infrared emission ceasing abruptly at the interface between the disk and the ring. The spiral arms of NGC 7714 and the bridge linking the two galaxies were not detected. On the LW3 map, the source IR1 does not coincide with any known optical counterpart, while the source IR2 on the LW6 map coincides with the radio source RGB J2336+021 (Laurent-Muehleisen et al., 1997).

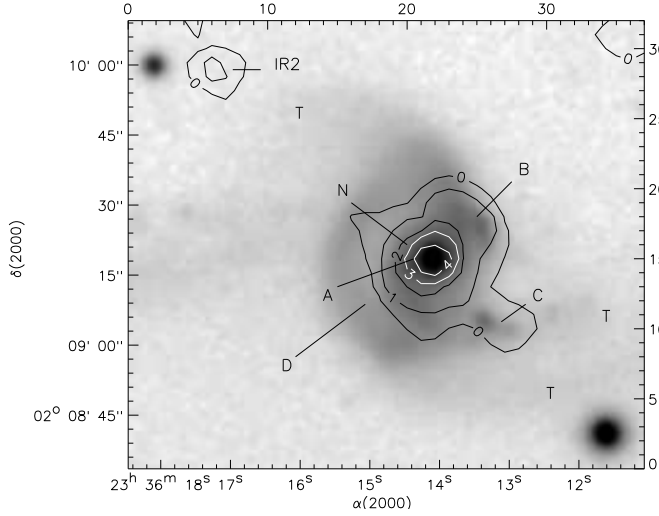


**Fig. 3.** Deconvolved LW6 map of NGC 7714, superimposed on a R band CCD image of NGC 7714. Contour levels ( $\text{mJy/arcsec}^{-2}$ ) are: 0 = 0.2, 1 = 1.0, 2 = 3.5, 3 = 9.0, 4 = 20.0. The map notation is the same as in Fig. 2. IR2 coincides with a weak radio source without an identified optical counterpart.

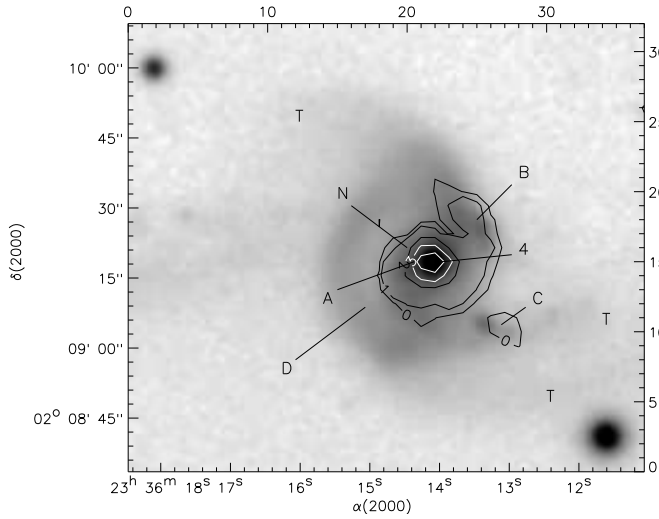


**Fig. 4.** LW9 map of NGC 7714. Contour levels ( $\text{mJy/arcsec}^{-2}$ ) are: 0 = 0.4, 1 = 1.0, 2 = 12.0, 3 = 33.0, 4 = 70.0. The map notation is the same as in Fig. 2. The nuclear region coincides with the strong LW9 emission.

The companion galaxy NGC 7715 was not detected in any of the three filter bands. Two weak sources were detected at the position of NGC 7715 in the LW3 filter in Fig. 1, but were determined to be glitches using robust deglitching techniques. The lack of emission from NGC 7715, along with the ring and spiral arms of NGC 7714 suggests that strong star formation is not present in these regions.

The PHOT-SL spectrum of NGC 7714 is presented in Fig. 5. Strong detections were made of unidentified in-

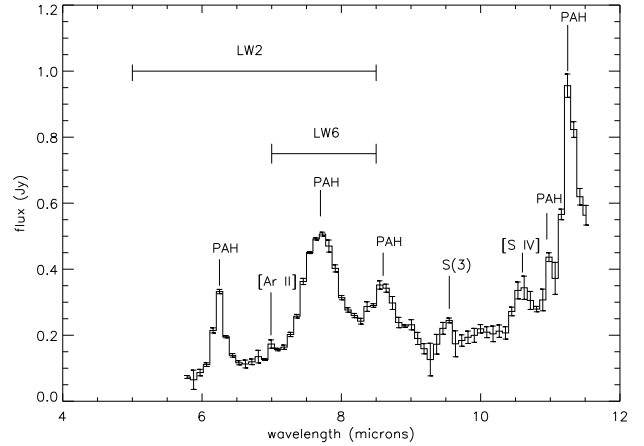


**Fig. 5.** Unsmoothed PHOT-SL spectrum of NGC 7714. The PAH features, along with [Ar II], [S IV] and the S(3) ground vibrational state of molecular hydrogen at  $9.66 \mu\text{m}$  are indicated. The bandpasses for the LW2 and LW6 ISOCAM filters are also indicated.

**Table 3.** PHOT-S fluxes for NGC 7714. The three columns give the line identification, the wavelength range and the integrated flux respectively.

line ID	Wavelength range ( $\mu\text{m}$ )	flux ( $10^{-15} \text{ W m}^{-2}$ )
PAH $6.2 \mu\text{m}$	6.0 - 6.6	$2.73 \pm 0.46$
[Ar II] $6.99 \mu\text{m}$	6.8 - 7.2	$0.74 \pm 0.10$
PAH $7.7 \mu\text{m}$	7.2 - 8.3	$8.84 \pm 1.10$
PAH $8.6 \mu\text{m}$	8.3 - 8.9	$1.22 \pm 0.24$
H <sub>2</sub> $9.66 \mu\text{m}$	9.3 - 9.9	$0.78 \pm 0.20$
[S IV] $10.5 \mu\text{m}$	10.4 - 10.8	$0.32 \pm 0.08$
PAH $11.0 \mu\text{m}$	10.8 - 11.1	$0.23 \pm 0.07$
PAH $11.3 \mu\text{m}$	11.1 - 11.6	$1.28 \pm 0.26$

frared bands (UIBs) at  $6.2$ ,  $7.7$ ,  $8.6$  and  $11.3 \mu\text{m}$  that are usually attributed to polycyclic aromatic hydrocarbons (PAHs) (Allamandola et al., 1989). A weak additional feature at  $11.0 \mu\text{m}$  may also be PAH (Moutou et al., 1999). The  $11.3 \mu\text{m}$  feature is quite strong relative to the  $7.7 \mu\text{m}$ , with a flux ratio of 2:1. [Ar II] was detected at  $6.99 \mu\text{m}$  in the unsmoothed spectrum at the  $3 \sigma$  level. Two weak features were also detected at about  $9.66$  and  $10.6 \mu\text{m}$ . The  $9.66 \mu\text{m}$  feature may be due to the S(3) pure rotational line,  $v = 0-0$ , of molecular hydrogen, while the  $10.6 \mu\text{m}$  feature may be a blend of [S IV] at  $10.51 \mu\text{m}$  and an additional unidentified component at  $10.6 \mu\text{m}$  to account for the width of the feature. The interpolated continuum between the ends of the wavelength range was subtracted to obtain the line fluxes. The identified line features and line fluxes are given in Table 3.

The spectral energy distribution of NGC 7714 using ISOCAM, PHT-SL and IRAS fluxes is presented in Fig.

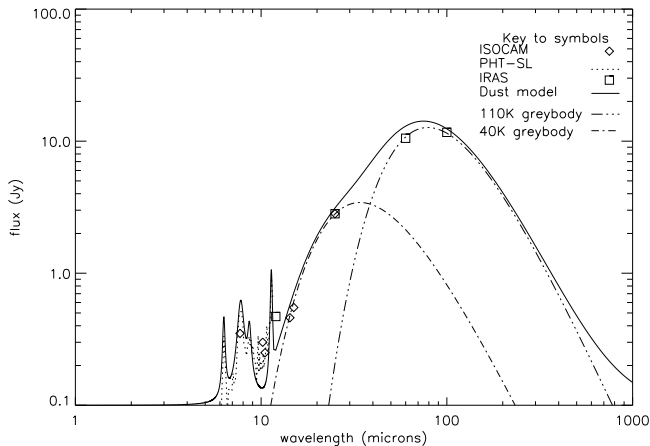


**Fig. 6.** Spectral energy distribution of NGC 7714 using ISO and IRAS flux data, including the key for the different symbols. The models are described in the text.

6. The dust model, denoted by the solid curve (Krugel & Siebenmorgen, 1994; Siebenmorgen et al., 1998), contains three separate dust populations: the PAH bands (Boulanger et al., 1998), a warm dust component at 110 K and a cooler dust component at 40 K and each component is indicated in the figure.

#### 4. Discussion

In order to explain the observed morphology and kinematics, Smith & Wallin (1992) modelled the Arp 284 system using an off-centre parabolic collision between two disk galaxies with a mass ratio  $M_2/M_1 \sim 0.3$ . The interaction occurred  $\sim 1.1 \times 10^8$  years ago, with the intruder galaxy impacting at a distance of 0.85 times the radius of the target disk. This model successfully reproduced the observed morphology, including the partial ring and the bridge linking the two galaxies. Further modelling (Smith et al., 1997) showed the bridge to be a hybrid between the tidal bridges observed in systems such as M 51 and gaseous 'splash' bridges such as that in the 'Taffy' interacting system VV 254 (Jarrett et al., 1999). The 'Taffy' system, which is at a comparable distance of 58.4 Mpc, is intrinsically bright in the mid-infrared and consists of three principal morphological infrared components: two multi-peaked nuclear regions, a large scale ring or wrapped spiral arm and a bridge linking the two galaxies which contains one quarter of the total H I in the system and has a significant dust content (Jarrett et al., 1999). Unlike the 'Taffy' system however, the bridge linking NGC 7714 and NGC 7715 was not detected in any of our three ISOCAM bands. Both Arp 284 and the 'Taffy' system have comparable HI column densities (Smith et al., 1997), but the lack of detectable emission from the bridge of Arp 284 indicates a low warm dust content. Further observations at longer wavelengths are required to determine the extent of the cold dust component.

The partial ring within NGC 7714, populated by red giant stars like those found in the companion galaxy, seems to be deficient in warm dust and is not detectable in the CAM maps. The model of Smith & Wallin (1992) may explain the lack of ongoing star formation within the partial ring of NGC 7714. In more central impacts, occurring at less than 0.2 times the radius of the target disk, the resulting strong radial oscillations lead to the formation of rings similar to those observed in the Cartwheel and Arp 10 (Charmandaris et al., 1999). Smith et al. (1997) noted that the optical ring in NGC 7714 does not have a prominent H I counterpart, similar to that found in the non star-forming inner ring of the Cartwheel but not in the outer ring (Higdon, 1996). Such differentiation of gas and stars is expected in partial rings formed during very off-center collisions. Thus, the lack of an H I counterpart does not rule out a collisional origin for the NGC 7714 ring. Another possibility is that the stellar ring may be a wrapped-around spiral arm caused by a noncollisional prograde planar encounter, rather than a collisional ring. The high column density of gas in the bridge, however, and its offset from the stars (Smith et al., 1997), supports the concept that gas was forced out of the main galaxy by a collision between two gas disks rather than merely perturbed in a grazing or long-range encounter.

The age of Wolf-Rayet stars in the central burst of NGC 7714 has been dated at between 4 and 5 Myr (Garcia-Vargas et al., 1997), yet this age is far short of the  $\sim 10^8$  years since the interaction. Given the amount of time since the onset of the interaction, any burst of star formation initiated by the interaction should have long since ceased, for example the companion galaxy NGC 7715, which has been in a post starburst phase for the last 50 - 70 Myr (Bernlohr, 1993). For such a young burst, gas infall to the nucleus must be ongoing to power the burst, and indeed HI gas may be falling from the bridge to the nuclear region (Papaderos & Fricke, 1998; Smith & Wallin, 1992). In a survey of 10 interacting galaxies, Bushouse et al. (1998) noted that galaxies similar in morphological type to NGC 7714 possessed nuclear infrared sources that are 10-100 times brighter than normal galaxies in the mid-infrared and have high levels of star formation. The companion galaxies, such as NGC 7715, have passed through their own star formation epoch and now lack the gas and dust to support large-scale star formation.

It is interesting to note that the ratio of LW3/LW2, where LW3 emission is dominated by dust and LW2 by PAHs, varies depending on the separation between the interacting galaxies (Hwang et al., 1999). The LW3/LW2 ratio generally decreases as interactions develop, starbursts age and separations increase (Vigroux et al., 1999; Cesarsky & Sauvage, 1999; Charmandaris et al., 1999). To determine the LW3/LW2 ratio for NGC 7714, the LW2 flux was synthesized from the PHOT-SL spectrum in the equivalent range of wavelengths to the ISOCAM LW2 filter, 5 to 8.5  $\mu\text{m}$ . In order to check the accuracy of the

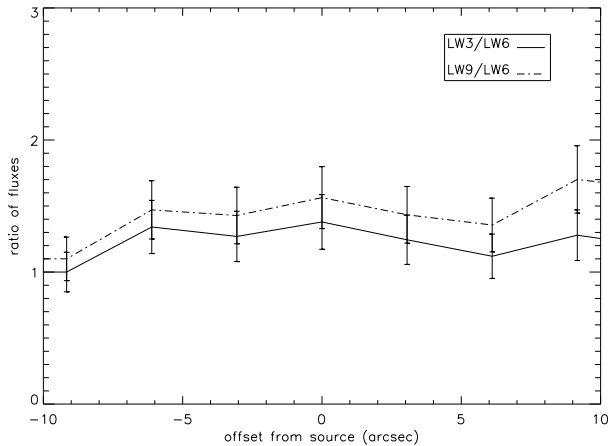


**Fig. 7.** Ratios of ISOCAM emission profiles in three filters obtained from the NE to SW scan across NGC 7714 at PA = 45°. The solid line gives the LW3/LW6 ratio, while the dot-dash line gives the LW9/LW6 ratio, and the 1 $\sigma$  error bars are included.

LW2 flux, LW2 and LW6 fluxes were obtained for several sources, including Mkn 297 and NGC 1741, from their PHOT-S spectra and the derived values agree with the respective ISOCAM fluxes within the photometric uncertainties. For NGC 7714, the LW3/LW2 ratio was  $1.5 \pm 0.2$ . This is quite low, since a ratio above 3 is indicative of high star formation due to the heating of dust in the nuclear region by hot, young ionising stars (Vigroux et al., 1999).

Since the LW3 and LW9 fluxes are dominated by dust emission, and the LW2 and LW6 by PAHs, the LW3/LW6 and LW9/LW6 ratios provide diagnostics similar to the LW3/LW2 ratio, allowing a determination of the current state of the starburst. To determine the LW9/LW6 and LW3/LW6 ratios, pixel fluxes were obtained in strips on each of the three raster maps, each strip bisecting NGC 7714 through the nuclear region. Each strip was equally separated by a position angle (PA) of 45°, measured from north, where PA = 0°. The strips were then divided to obtain LW9/LW6 and LW3/LW6 ratios. One such strip is presented in Fig. 7, taken from northwest to southeast through the galaxy. The LW9/LW6 and LW3/LW6 ratios were quite low, with values falling between 1 and 1.7. Combining these findings with the low value of  $1.5 \pm 0.2$  for the LW3/LW2 ratio, it may be that while the nuclear region of NGC 7714 is still in the throes of a young starburst indicated by the Wolf-Rayet features, the low ratio values along with the age of the burst suggest that NGC 7714 is moving into a post-starburst stage (Charmandaris et al., 1999). The aging of the burst may be due to supernovae and stellar winds (Taniguchi & Kawara, 1988) disrupting the interstellar medium, preventing further star formation as soon as the first generation of O stars have formed and evolved (Cesarsky & Genzel, 2000).

The 11.3  $\mu\text{m}$  PAH feature is quite strong relative to the 7.7  $\mu\text{m}$  PAH feature. This ratio is particularly sensitive to the degree of ionization, implying that the detected PAHs may not have been ionized. A strong 11.3  $\mu\text{m}$  feature is common in colder galaxies like NGC 7714, since it is linked to neutral PAHs and is indicative of a high degree of hydrogenation in the PAHs (Peeters et al., 1999; Lu et al., 1999). PAHs exposed to a harder radiation field, for example within the H II regions and on the interface between the H II and the molecular cloud, can be ionized, loose hydrogen atoms and/or disappear by photodissociation. Proximity to highly ionizing sources, such as young O stars within a burst may thus lead to dehydrogenation of the PAHs. Moving out past the H II/molecular cloud interface, the degree of hydrogenation increases (Verstraete et al., 1996; Roelfesma et al., 1996).

The compact nature of the nucleus of NGC 7714 and its extremely high surface brightness (Weedman et al., 1998) have led to suspicions that NGC 7714 harbours an active nucleus. While the galaxy has far-infrared IRAS colours more in line with Seyfert 2 galaxies than starbursts (Gonzalez-Delgado et al., 1994), the emission lines of H $\alpha$ , [NII]  $\lambda\lambda 6548, 6583$ , [SII]  $\lambda\lambda 6716, 6731$ , He I  $\lambda 5876$  and [OI]  $\lambda 6300$  are not broad enough to suggest the presence of a Seyfert nucleus (Demoulin et al., 1968). UV observations by the HST (Gonzalez-Delgado et al., 1999) have shown that the nuclear region contains  $\sim 2000$  Wolf-Rayet and 20000 O type stars, with an age for the burst of 4 to 5 Myr, while ROSAT (Papaderos & Fricke, 1998; Stevens & Strickland, 1998) has shown it to be a strong X-ray source. The high excitation of material within the nuclear region can account for the 6.99  $\mu\text{m}$  [Ar II] line. The 9.6  $\mu\text{m}$  feature may be due to the S(3) ground vibrational molecular hydrogen ground state of molecular hydrogen. Ultraviolet fluorescence, excitation by low-velocity shocks and heating caused by X-rays are considered to be the primary emission mechanisms for the excitation of molecular hydrogen (Black & van Dishoeck, 1987; Draine & Robergse, 1982; Mouri, 1994). These mechanisms require a source of dense gas to be located near the source of illumination such as a starburst. Excitation may also occur due to slow shocks induced by jets or by kinetic processes such as winds, superwinds and supernovae. Spectroscopic studies of Seyfert galaxies indicate that no single process is responsible for the H $_2$  emission (Quillen et al., 1999).

Several diagnostic tools are available to probe the nature of the activity within the nuclear region. The ratio of the integrated PAH luminosity and the 40 to 120  $\mu\text{m}$  IR luminosity (Lu et al., 1999) provides a tool to discriminate between starbursts, AGN and normal galaxies because the lower the ratio, the more active the galaxy. For NGC 7714, the ratio is 0.09 and is consistent with the values found for other starbursts (Vigroux et al., 1999). Similarly, the ratio of the 7.7  $\mu\text{m}$  PAH flux to the continuum level at this wavelength can provide a measure of the level of activity within the nucleus (Genzel et al., 1998; Laureijs et al.,

2000). The ratio for NGC 7714 is 3.3 and is indicative of an active starburst. The results from these diagnostic tools indicate that NGC 7714 is home to a compact burst of star formation, and suggests that an AGN is not present within the nuclear region.

## 5. Conclusions

Deconvolved ISOCAM maps of the Arp 284 system were obtained with the LW3, LW6 and LW9 filters, with strong emission detected from the central source in NGC 7714. IR emission was not detected from the companion galaxy NGC 7715, the bridge linking the two galaxies or from the partial stellar ring, where emission ceases abruptly at the interface between the disk and the ring. ISOPHOT spectrometry of the nuclear region of NGC 7714 was also obtained, with strong PAH features, the emission line [Ar II], molecular hydrogen at  $9.66 \mu\text{m}$  and a blend of lines including [S IV] about  $10.6 \mu\text{m}$  all present within the spectrum.

The morphology of the system is well described by an off-centre collision between the two galaxies. A series of diagnostic tools allowed an investigation to be performed regarding the activity within the central region of NGC 7714. The LW3/LW2, where the LW2 flux was synthesized from PHOT-S measurements, LW9/LW6 and LW3/LW6 ratios suggest that the central burst within NGC 7714 is moving towards the post-starburst phase. The ratio of the integrated PAH luminosity to the 40 to  $120 \mu\text{m}$  infrared luminosity and the far-infrared colours reveal that despite the high surface brightness of the nucleus, the properties of NGC 7714 can be explained in terms of a starburst and do not require the presence an AGN.

*Acknowledgements.* We thank P. Papaderos and K. Fricke for kindly allowing the use of their CCD image of the Arp 284 system. The ISOCAM data presented in this paper was analysed using 'CIA', a joint development by the ESA Astrophysics Division and the ISOCAM Consortium. The ISOCAM Consortium is led by the ISOCAM PI, C. Cesarsky, Direction des Sciences de la Matière, C.E.A., France. The ISOPHOT data was reduced using PIA, which is a joint development by the ESA Astrophysics Division and the ISOPHOT consortium.

## References

- Abergel A., Bernard J.P., Boulanger F. et al., 1996, A&A 315, L329
- Acosta-Pulido J.A., Gabriel C., Castaeda H., 1999, accepted for publication in *Experimental Astronomy*, Kluwer Academic Publishers (1999)
- Allamandola L.J., Tielens A.G.G.M., Barker J., 1989, ApJS 71, 733
- Aussel H., Cesarsky C.J., Elbaz D. et al., 1999, A&A 342, 313
- Bernlohr K., 1993, A&A 268, L25
- Black J.H., van Dishoeck E.F., 1987, ApJ 322, 412
- Boulanger F., Boissel P., Cesarsky D. et al., 1998, A&A 339, 194
- Bushouse H., Telesco C.M., Warner M.W., 1998, AJ 115, 938
- Cesarsky C., Sauvage M., 1999, Kluwer Academic Publishers, in press
- Cesarsky C., Abergel A., Agnese P. et al., 1996, A&A 315, L32
- Cesarsky C., Genzel R., 2000, astro-ph 002184, Ann.Rev.Astron.Astrophys., in press
- Charmandaris V., Laurent O., Mirabel I.F. et al., 1999, In: Cox P., Kessler M.F. (eds) *The Universe as seen by ISO*, ESA SP-427, volume 2, p. 869
- Charmandaris V., Laurent O., Mirabel I.F. et al., 1999, In: Combes F., Manon G.A., Charmandaris V. (eds) *Galaxy Dynamics : from the Early Universe to the Present*, ASP Conference Series, in press
- Conti P.S., 1991, ApJ 377, 115
- Delaney M., 1998, ISOCAM Interactive Analysis User's Manual 3.0, ESA SAI/96-5226/DC
- Demoulin M.H., Burbridge E.M., Burbridge G.R., 1968, ApJ 153, 31
- Draine B.T., Roberge W.G., 1982, ApJ 259, L91
- Gabriel C., 1998, PHOT Interactive Analysis User Manual, ESA, <http://www.iso.vilspa.esa.es/manuals/>
- Garcia-Vargas M.L., Gonzalez-Delgado R.M., Perez E. et al., 1997, ApJ 478, 112
- Genzel R., Lutz D., Sturm E. et al., 1998, ApJ 498, 579
- Gonzalez Delgado R.M., Perez E., Diaz A.I. et al., 1994, ApJ 439, 604
- Gonzalez Delgado R.M., Garcia-Vargas M.L., Goldader J. et al., 1999, ApJ 513, 707
- Heisler C., De Robertis M., Nadeau D., 1996, MNRAS 280, 579
- Higdon J.L., 1996, ApJ 467, 241
- Hwang C.Y., Lo K.Y., Gao Y. et al., 1999, ApJ 511, 17
- Jarrett T.H., Helou G., Van Buren D. et al, 1999, In: Cox P., Kessler M.F. (eds) *The Universe as seen by ISO*, ESA SP-427, volume 2, p. 897
- Krugel E., Siebenmorgen R., 1994, A&A 282, 407
- Laurent-Muehleisen S.A., Kollgaard R.I., Ryan P.J. et al., 1997, A&AS 122, 235
- Laureijs R.J., Klaas U., Richards P.J. et al., 1998, ISOPHOT Data Users Manual, ESA, <http://www.iso.vilspa.esa.es/manuals/>
- Laureijs R., Watson D., Metcalfe L. et al., 2000, A&A in press
- Lemke D., Klaas U., Abolins J. et al., 1996, A&A 315, L64
- Lu N.Y., Helou G., Silbermann N. et al, 1999, In: Cox P., Kessler M.F. (eds), *The Universe as seen by ISO*, ESA SP-427, volume 2, p. 929
- Mas-Hesse J.M., Kunth D., 1999, A&A 349, 765
- Metcalfe L., Steel S., Barr P. et al., 1996, A&A 315, L105
- Moshir M., Kopan G., Conrow T. et al., 1990, In: *The Faint Source Catalog*, version 2.0, *Infrared Astronomical Satellite Catalogs*, Infrared Processing and Analysis

Centre

- Mouri H., 1994, *ApJ* 427, 777
- Moutou C., Sellgren K., Leger A. et al., 1999, In: d'Hendecourt L., Joublin C., Jones A., (eds) *Solid interstellar matter: the ISO revolution*, Les Houches Workshop, EDP Sciences and Springer-Verlag
- Ott S., Abergel A., Altieri B. et al. 1997, In: Hunt, G., Payne, H. (eds.), *Astronomical Data Analysis Software and Systems VI*, Vol. 125 of ASP Conf. Series, p. 34
- Papaderos C.P., Fricke K.J., 1998, *A&A* 338, L31
- Peeters E., Tielens A.G.G.M., Roelfesma P.R. et al, 1999, In: Cox P., Kessler M.F. (eds), *The Universe as seen by ISO*, ESA SP-427, volume 2, p. 739
- Quillen A.C., Alonso-Herrero A., Rieke M.J. et al., 1999, *ApJ* 527, 696
- Rigopoulou D., Genzel R., Lutz D. et al, 1999, In: Cox P., Kessler M.F. (eds), *The Universe as seen by ISO*, ESA SP-427, volume 2, p. 833
- Roelfesma P.R., Cox P., Tielens A.G.G.M. et al., 1996, *A&A* 315, 289
- Schaerer D., Vacca W.D., 1998, *AJ* 497, 618
- Schaerer D., Contini T., Pindao M., 1999, *A&AS* 136, 35
- Siebenmorgen R., Krugel E., Chini R. 1998, *A&A* 351, 495
- Siebenmorgen R., Blommaert J., Sauvage M. et al., 1999, In: *ISO Handbook Volume III (CAM)*, Version 1.0 ESA SAI-99-057/Dc, Version 1.0 July 16, 1999, <http://www.iso.vilspa.esa.es/manuals/>
- Smith B., Wallin J.F. 1992, *ApJ* 393, 544
- Smith B., Struck J., Pogge R., 1997, *ApJ* 483, 754
- Starck J., Murtagh F., Bijaoui A., 1998, In: *Image Processing and Data Analysis: The Multiscale Approach*, Cambridge Univ. Press
- Stevens I., Strickland D., 1998, *MNRAS* 294, 523
- Storchi-Bergmann T., Fernandes R.D., Schmitt H.R., 1998, *ApJ* 501, 94
- Taniguchi Y., Kawara K., 1988, *AJ* 95, 1378
- Van Breugel W., Filippenko A.V. , Heckman T. et al., 1985, *ApJ* 293, 83
- Verstraete L., Puget J.L., Falgarone E. et al., 1996, *A&A* 315, 337
- Vigroux L., Charmandais V., Gallais P. et al, 1999, In: Cox P., Kessler M.F. (eds), *The Universe as seen by ISO*, ESA SP-427, volume 2, p. 805
- Weedman D.W., Feldman F.R., Balzano V.A. et al., 1981, *ApJ* 248, 105
- Weedman D.W., Wolovitz J.B., Bershady M.A. et al, 1998, *AJ* 116, 1643